Received: 11 March 2021 | Revised: 17 August 2021 | Accepted: 18 August 2021

DOI: 10.1111/mpp.13134

Molecular Plant Pathology WILEY

ORIGINAL ARTICLE

Activation of the BABA-induced priming defence through redox homeostasis and the modules of TGA1 and MAPKK5 in postharvest peach fruit

Chunhong Li[1,2] | Kaituo Wang[1,2] | Yixiao Huang[3] | Changyi Lei[1] | Shifeng Cao[4] | Linglan Qiu[1] | Feng Xu[2,5] | Yongbo Jiang[1] | Yanyu Zou[1] | Yonghua Zheng[2]

[1]College of Biology and Food Engineering, Chongqing Three Gorges University, Chongqing, China

[2]College of Food Science and Technology, Nanjing Agricultural University, Nanjing, China

[3]College of Art and Science, University of Miami, Coral Gables, Florida, USA

[4]College of Biological and Environmental Sciences, Zhejiang Wanli University, Ningbo, China

[5]College of Food and Pharmaceutical Sciences, Ningbo University, Ningbo, China

Correspondence
Kaituo Wang, College of Biology and Food Engineering, Chongqing Three Gorges University, Chongqing, China.
Email: wangkaituo83@gmail.com

Funding information
National Natural Science Foundation of China, Grant/Award Number: 31671913 and 31672209; Natural Science Foundation of Ningbo City, Grant/Award Number: 2018A610224; Funds for Innovative Research Groups of University in Chongqing City, Grant/Award Number: CXQT21036

Abstract

The priming of defence responses in pathogen-challenged model plants undergoes a preparation phase and an expression phase for defence function. However, the priming response in postharvest fruits has not been elucidated. Here, we found that 50 mM β-aminobutyric acid (BABA) treatment could induce two distinct pathways linked with TGA1-related systemic acquired resistance (SAR), resulting in the alleviation of Rhizopus rot in postharvest peach fruit. The first priming phase was elicited by BABA alone, leading to the enhanced transcription of redox-regulated genes and posttranslational modification of PpTGA1. The second phase was activated by an H_2O_2 burst via up-regulation of *PpRBOH* genes and stimulation of the MAPK cascade on pathogen invasion, resulting in a robust defence. In the MAPK cascade, PpMAPKK5 was identified as a shortcut interacting protein of PpTGA1 and increased the DNA binding activity of PpTGA1 for the activation of salicylic acid (SA)-responsive *PR* genes. The overexpression of *PpMAPKK5* in *Arabidopsis* caused the constitutive transcription of SA-dependent *PR* genes and as a result conferred resistance against the fungus *Rhizopus stolonifer*. Hence, we suggest that the BABA-induced priming defence in peaches is activated by redox homeostasis with an elicitor-induced reductive signalling and a pathogen-stimulated H_2O_2 burst, which is accompanied by the possible phosphorylation of PpTGA1 by PpMAPKK5 for signal amplification.

Abbreviations: 6PGDH, 6-phosphaogluconate dehydrogenase; AbA, aureobasidin A; APX, ascorbate peroxidase; AsA-GSH, ascorbic acid-glutathione; BA2H, benzoic acid 2-hydroxylase; BABA, β-aminobutyric acid; BLAST, basic local alignment search tool; BTH, benzothiadiazole; CAT, catalase; Co-IP, coimmunopreicipitation; CRISPR, clustered regularly interspaced short palindromic repeats; DDO, double dropout medium; DHAR, dehydroascorbate reductase; DLR, dual-luciferase reporter; dpi, days postinoculation; dscDNA, double-stranded cDNA; ET, ethylene; ETI, effector-triggered immunity; G6PDH, glucose-6-phosphate dehydrogenase; GR, glutathione reductase; GST, glutathione; H_2O_2, hydrogen peroxide; His, histidine; ISR, induced systemic resistance; iTOL, interactive tree of life; JA, jasmonic acid; MAPK, mitogen-activated protein kinase; MDHAR, monodehydroascorbate reductase; MEGA, Molecular Evolutionary Genetics Analysis; MS, Murashige and Skoog; NADPH, reduced coenzyme II; NCBI, National Center for Biotechnology Information; NJ, neighbour-joining; NPR1, nonexpressor of pathogenesis-related genes 1; PAMPs/MAMPs, pathogen- or microbe-associated molecular patterns; PBS, phosphate-buffered saline; PDA, potato dextrose agar; PGLS, 6-phosphogluconolactonase; PGPR, plant-growth-promoting rhizobacteria; POD, peroxidase; PPP, pentose phosphate pathway; *PR*, pathogenesis-related gene; PRRs, pattern-recognition receptors; PTI, pattern-triggered immunity; QDO, quadruple dropout medium; qPCR, quantitative PCR; RBOH, respiratory burst oxidase homologue; ROS, reactive oxygen species; SA, salicylic acid; SAR, systemic acquired resistance; SD/−Leu−Trp, synthetic dropout medium lacking leucine and tryptophan; SD/−Leu−Trp−His, synthetic dropout medium lacking leucine, tryptophan, and histidine; SD/−Leu−Trp−His−Ade, synthetic dropout medium lacking leucine, tryptophan, histidine, and adenine; SMART, simple modular architecture research tool; SOD, superoxide; TAL, transaldolase; TBtools, toolkit for biologists; TDO, triple dropout medium; TFs, transcription factors; TKT, transketolase; WT, wild-type; XTT, 3′-[1-(phenylamino-carbonyl)-3,4-tetrazolium]-bis(4-methoxy-6-nitro) benzenesulfonic acid hydrate; X-α-gal, X-α-D-galactosidase; Y1H, yeast one-hybrid; Y2H, yeast two-hybrid.

This is an open access article under the terms of the Creative Commons Attribution-NonCommercial-NoDerivs License, which permits use and distribution in any medium, provided the original work is properly cited, the use is non-commercial and no modifications or adaptations are made.
© 2021 The Authors. *Molecular Plant Pathology* published by British Society for Plant Pathology and John Wiley & Sons Ltd.

KEYWORDS
MAPKK, peach, priming resistance, redox, *Rhizopus stolonifer*, TGA1, β-aminobutyric acid

1 | INTRODUCTION

To effectively defend against invading pathogenic microorganisms, plants have evolved intricate mechanisms that have given rise to multilayered and tightly controlled signalling networks of constitutive and induced resistance (Glazebrook, 2005). The first layer, referred to as pathogen-associated molecular pattern-triggered immunity (PTI), is performed by the specific recognition of plasma membrane-localized pattern recognition receptors (PRRs) by pathogen-associated molecular patterns (PAMPs)/microbe-associated molecular patterns (MAMPs) and is characterized by an oxidative burst, rapid MAPK activation, callose deposition, stomatal closure, and PTI-responsive gene transcription within minutes of PAMP/MAMP perception (Gust et al., 2007; Zipfel & Robatzek, 2010). Plants have also evolved a second level of innate immunity, called effector-triggered immunity (ETI), which depends on the specific recognition of pathogen effectors by host resistance (*R*) proteins, leading to hypersensitive cell death at the site of pathogen infection to confine the spread of pathogens (Coll et al., 2011). Salicylic acid (SA)-dependent systemic acquired resistance (SAR) also confers long-lasting resistance to a wide spectrum of pathogen challenges (Vallad & Goodman, 2004). SA signalling is related to the proper activation of the majority of SA-inducible genes during PTI, and the transcription of SA response marker genes in *R* protein-mediated ETI can be partly regulated in an SA-dependent manner (Glazebrook, 2005; Tsuda et al., 2013). SAR is usually accompanied by SA-dependent defence responses via an NPR1-dependent mechanism and results in resistance predominantly against biotrophic pathogens (Dong, 2004; Ton et al., 2002). Another defence system, induced systemic resistance (ISR), can be triggered by the colonization of plant roots by plant growth-promoting rhizobacteria (PGPR) and can be regulated by jasmonic acid (JA) and ethylene (ET) signalling pathways (Pieterse et al., 2000; Verhagen et al., 2004). Over the decades, priming has been documented as a universal feature of the plant immune response that confers SAR/ISR against pathogenic threats (Conrath et al., 2006). For example, SA and its analogue benzothiadiazole (BTH) can prime *Arabidopsis* for potentiated transcription of SA-responsive *PR* genes (Kohler et al., 2002). A mutation-based experiment indicated a crucial role of NPR1 in the SA-signalling priming defence (Canet et al., 2010). ISR induced by the PGPR *Pseudomonas fluorescens* WCS374 was determined to prime JA- and/or ET-regulated defence genes in *Arabidopsis* against further pathogen attack (Pozo et al., 2008). β-aminobutyric acid (BABA), a nonproteinogenic amino acid, exerts inducible effects by priming a SAR defence with SA-signalling *PR* gene transcription and/or SA-independent callose deposition at infected sites (Cohen et al., 2016). In our previous studies, after treatment with a suitable concentration of BABA (ranging from 10 to 50 mM), fruits, such as peach (*Prunus persica*), strawberry (*Fragaria* × *ananassa*), and table grape (*Vitis vinifera*), were found to enter a special physiological condition, referred to as the primed state, that enabled them to remain dormant under low disease pressure but respond in a more rapid and robust manner to a considerably higher grade of stimulus than nonprimed fruits (Li et al., 2020c, 2021; Wang et al., 2016, 2019, 2021). Nevertheless, the identity of the key regulatory node underlying BABA-induced priming resistance remains unclear.

Rhizopus stolonifer is a necrotrophic fungal pathogen, and Rhizopus soft rot caused by the pathogen on the succulent tissues of vegetables, fruits, and ornamentals usually occurs during the postharvest period. After harvest, *R. stolonifer* is omnipresent as a saprophyte and sometimes as a plant parasite (Kwon & Lee, 2006). Specifically, Rhizopus rot is one of the dominant postharvest mould diseases in peach, resulting in great loss after harvest (Baggio et al., 2017). Previously, we revealed that protection of peach fruit by BABA against the invasion of the fungal pathogen *R. stolonifer* was accompanied by the transcript accumulation of nuclear-translocated TGA1, a key redox-controlled factor of SAR, which is essential for the activation of priming resistance in postharvest peach fruit (Li et al., 2020b). The MAPK signalling cascade, a highly conserved eukaryotic pathway featuring a distinct cascade of three successive phosphorylation events, is involved in the phosphorylation of certain specific transcription factors (TFs) and eventually converts external stimulations into intracellular responses. The MAPK cascade serves as the convergence point of multiple signalling transduction pathways (Jonak et al., 2002; Mutalik & Venkatesh, 2006; Sugiura et al., 1999). Nevertheless, whether or not the regulatory role of the MAPK cascade is intertwined with TGA1 in the BABA-induced priming response remains unknown. In a preliminary trial, a novel group C MAPK kinase of PpMAPKK5 was identified as a PpTGA1 binding partner that was positively involved in induced resistance against *R. stolonifer* in peaches. Herein, we elucidated the role of BABA in inducing SAR-related priming resistance in peach fruit and provided a broad picture of the switch between the primed state and activation of the priming defence.

2 | RESULTS

2.1 | Inhibitory effect of BABA elicitation against *R. stolonifer* infection in peaches

Peaches are susceptible to Rhizopus soft rot caused by the fungus *R. stolonifer*, as depicted in Figure 1a,b. Pretreatment with 50 mM BABA resulted in significant suppression of disease severity in peaches, and the lesion diameter and disease occurrence were 28.28% and 26.44%, respectively, lower than those of peaches

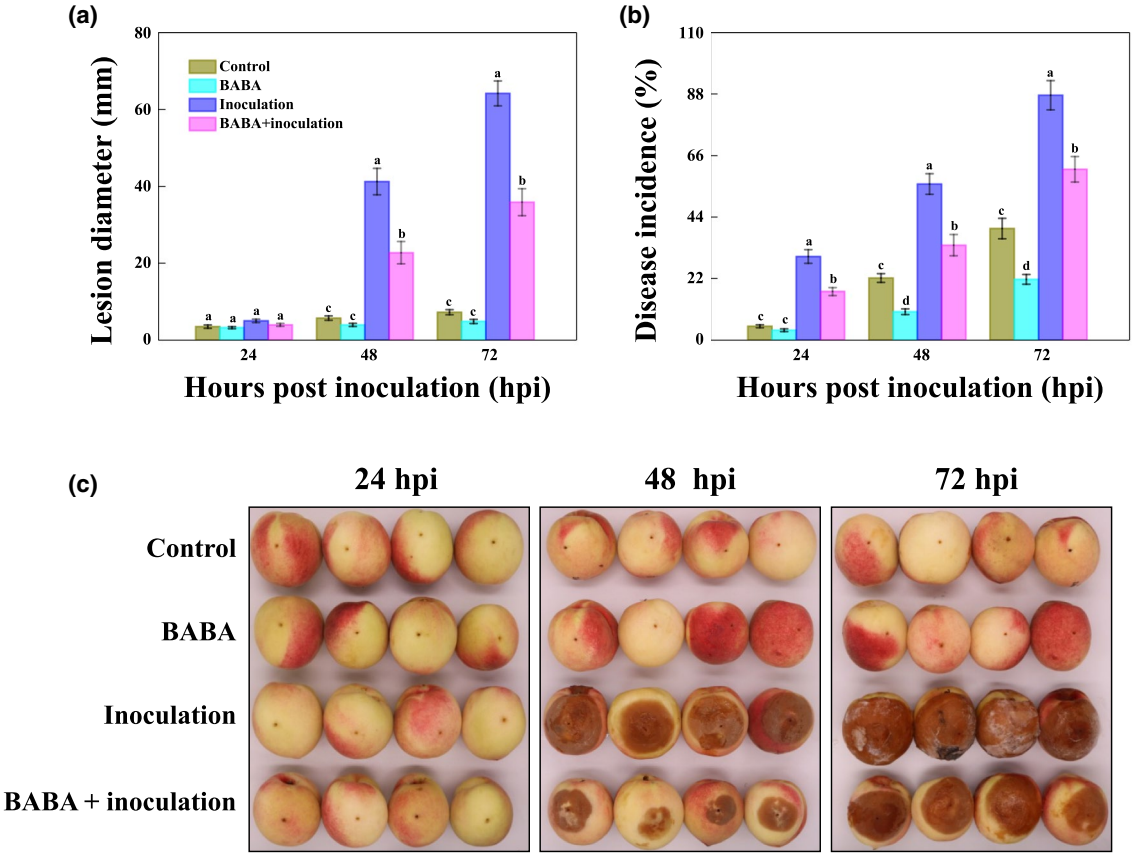

FIGURE 1 BABA elicitation retarded disease development in peaches inoculated with the fungal pathogen *Rhizopus stolonifer*. (a) Lesion diameter, (b) disease incidence, and (c) visual appearance measured at 24 hr intervals after inoculation of peach fruit with *R. stolonifer*. Peaches were dot-inoculated with double-deionized water (purple bars) or 50 mM BABA (pink bars) before inoculation with *R. stolonifer*. Lesion diameter and disease incidence were recorded as the mean ± *SE*. Different lowercase letters above the bar indicate a significant ($p < 0.05$) difference among BABA-treated, *R. stolonifer*-inoculated, and control peaches. Representative peaches were photographed and compared at 24, 48, and 72 hr postinoculation (hpi) of storage at 20°C

inoculated with *R. stolonifer* alone at 72 hr postinoculation (hpi). Notably, treatment with 50 mM BABA clearly retarded the occurrence of brown-rot decay and/or black-and-white hyphae on the surface of fruit pericarps, especially at 48 and 72 hpi (Figure 1c).

2.2 | Effect of BABA elicitation on the regulation of redox status in peaches

As shown in Figure 2, higher transcript levels of genes encoding key enzymes related to the ascorbate-glutathione (AsA-GSH) cycle (GR, DHAR, MDHAR, and APX), reactive oxygen species (ROS) system (SOD, CAT, and POD), and pentose phosphate pathway (PPP; G6PDH, 6PGDH, PGLS, TKT, and TAL) in sole *R. stolonifer*-inoculated or BABA-treated peaches could be observed compared with those in the controls. In all BABA-pretreated samples, transcript levels of these genes involved in the AsA-GSH cycle, ROS system, and PPP generally peaked at approximately 12–24 hpi, followed by gradual decrease. The involvement of the potentiated transcription of critical genes in the AsA-GSH cycle, ROS system, and PPP in BABA-pretreated peaches with subsequent pathogen inoculation was in agreement with our previous observations of their activities (Li et al., 2020b). As a consequence, BABA stimulated the redox potential of the fruit cells towards a highly reductive condition on their perception of pathogen invasion.

2.3 | Effect of BABA elicitation on H_2O_2 burst and SA-dependent defence response in peaches

The BABA-elicited SAR of peach fruit against *R. stolonifer* was observed along with an oxidative burst, as demonstrated by the potentiation of NADPH oxidase activity, the transcription of *PpRBOH*s and the accumulation of H_2O_2 content (Figure 3a–c). Moreover, BABA-mediated protection of peaches against *R. stolonifer* activated the transcription of *PpMAPKKK5*s and *PpMAPKK5* (Figure 3c). The effect of BABA on the mRNA transcripts of SA biosynthesis genes (PAL, ICS, CM, BA2H, and IPL), NPR1 (a master regulator of SAR), and SA-responsive genes, such as *PpPR1*s, *PpPR2*s, and *PpPR5*s, of peaches infected by *R. stolonifer* is presented in Figure 3d. All of

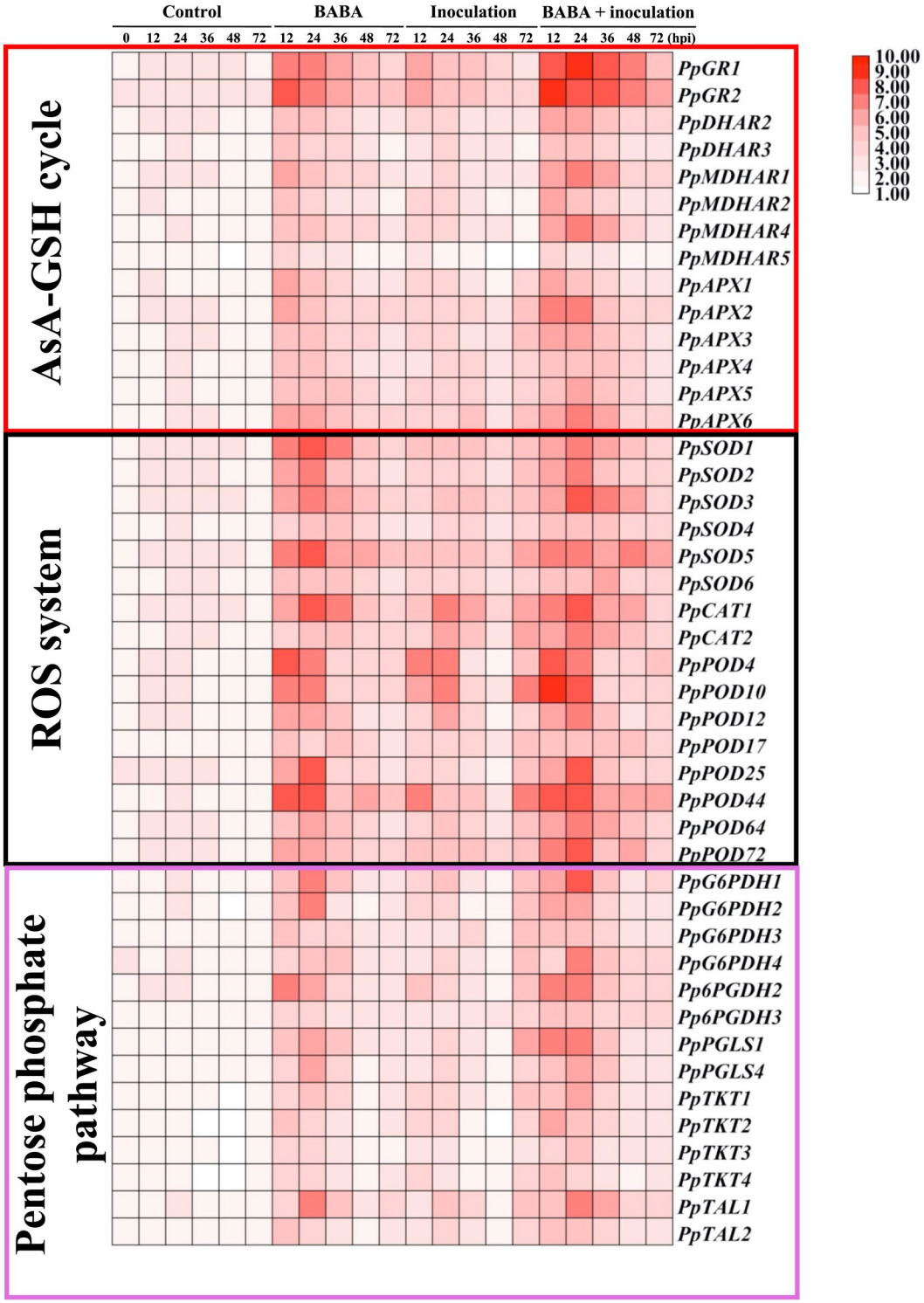

FIGURE 2 Transcript levels of key enzymes associated with the ascorbic acid-glutathione (AsA-GSH) cycle, reactive oxygen species (ROS) system, and pentose phosphate pathway in peaches after inoculation with *Rhizopus stolonifer* at 12 hr intervals. mRNA transcripts were profiled by quantitative reverse transcription PCR and visualized with a heatmap, in which peach *TEF2* was used as an internal standard. Data represent means from six measurements

the SA biosynthesis genes began to show transcript accumulation as soon as BABA treatment was applied, and their expression was highly induced following inoculation with *R. stolonifer*. In addition, BABA-primed SAR responses against *R. stolonifer* invasion were observed by analysing the transcription of the *PpNPR1* and SA-responsive *PpPR1*, *PpPR2*, and *PpPR5* genes, and the observed kinetics and intensity were similar to those of the transcript profile of *PpMAPKKK5*s/*PpMAPKK5* (Figure 3c,d).

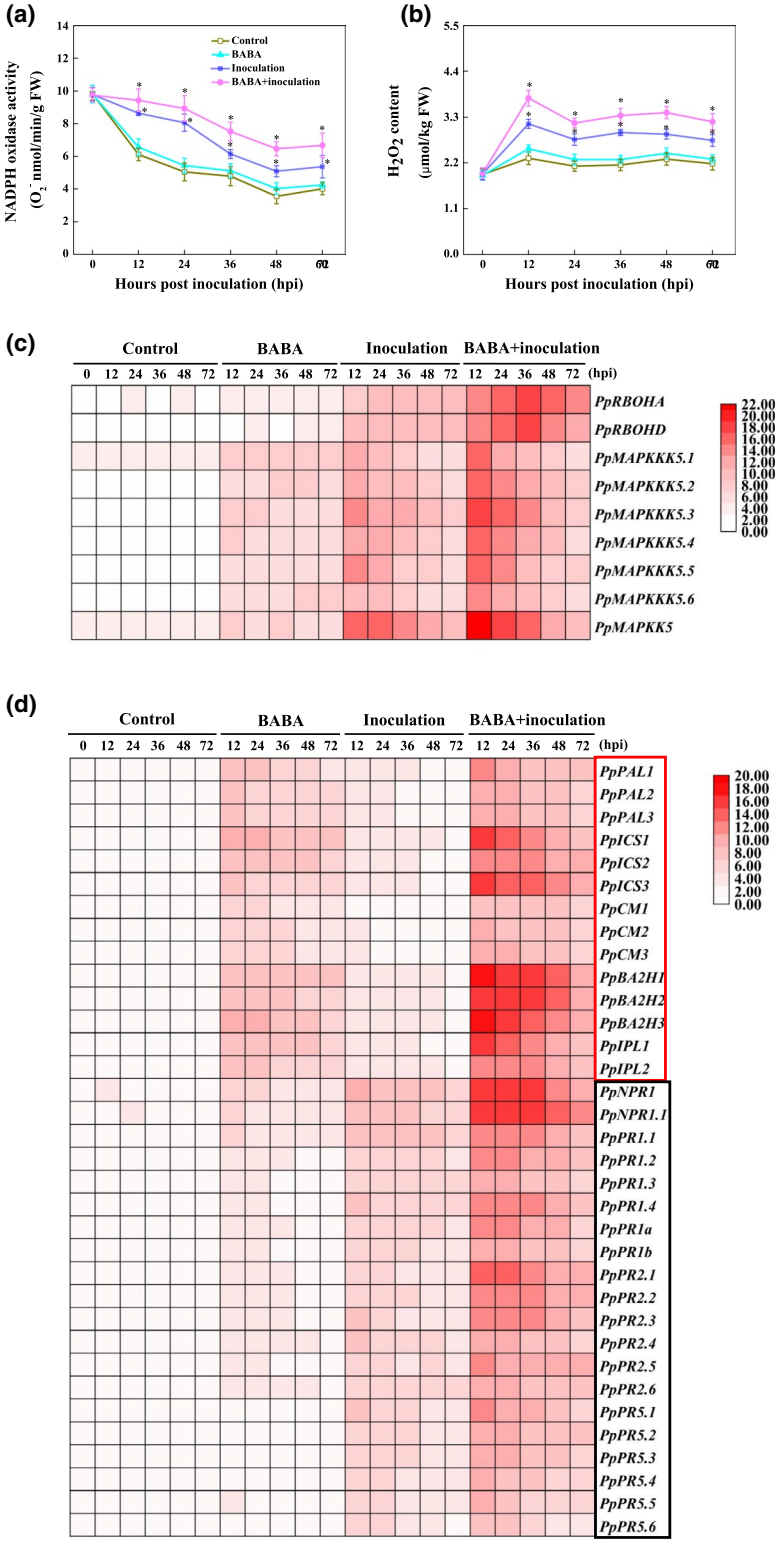

FIGURE 3 Changes in NADPH oxidase activity, H_2O_2 content and transcript levels of *PpMAPKKK5*s/*PpMAPKK5*, salicylic acid (SA) biosynthesis, and SA-responsive genes in peaches after inoculation with *Rhizopus stolonifer* at 12 hr intervals. NADPH oxidase activity (a) and H_2O_2 content (b) were recorded as the mean ± *SE*. Asterisks indicate significant ($p = 0.05$ level) differences among BABA-treated, *R. stolonifer*-inoculated, and untreated peaches. mRNA expression levels, including *PpMAPKKK5*s/*PpMAPKK5* (c) and SA biosynthesis and SA-responsive genes (d), were profiled using quantitative reverse transcription PCR and visualized with heatmap. Peach *TEF2* was used as an internal standard. Data represent means from six measurements

2.4 | Screening for PpTGA1-interacting proteins from peach fruit

As shown in Figure S1, after double selection on TDO plates supplemented with 10 or 20 mM 3-AT, a total of 205 single colonies were selected. The library plasmids were transformed into *Escherichia coli* DH5α for colony PCR, sequencing, and searching with BlastN (nucleotide BLAST), where 89 single colonies were amplified and 61 positive colonies were successfully sequenced. A total of 53 different coding sequences from BLAST alignments were eventually obtained. Further verification showed that only 34 positive colonies were present on double verification plates (TDO + 10/20 mM 3-AT). Notably, one colony (no. 158) was homologous with *P. persica* mitogen-activated protein kinase kinase 5 (MAPKK5, LOC18781583).

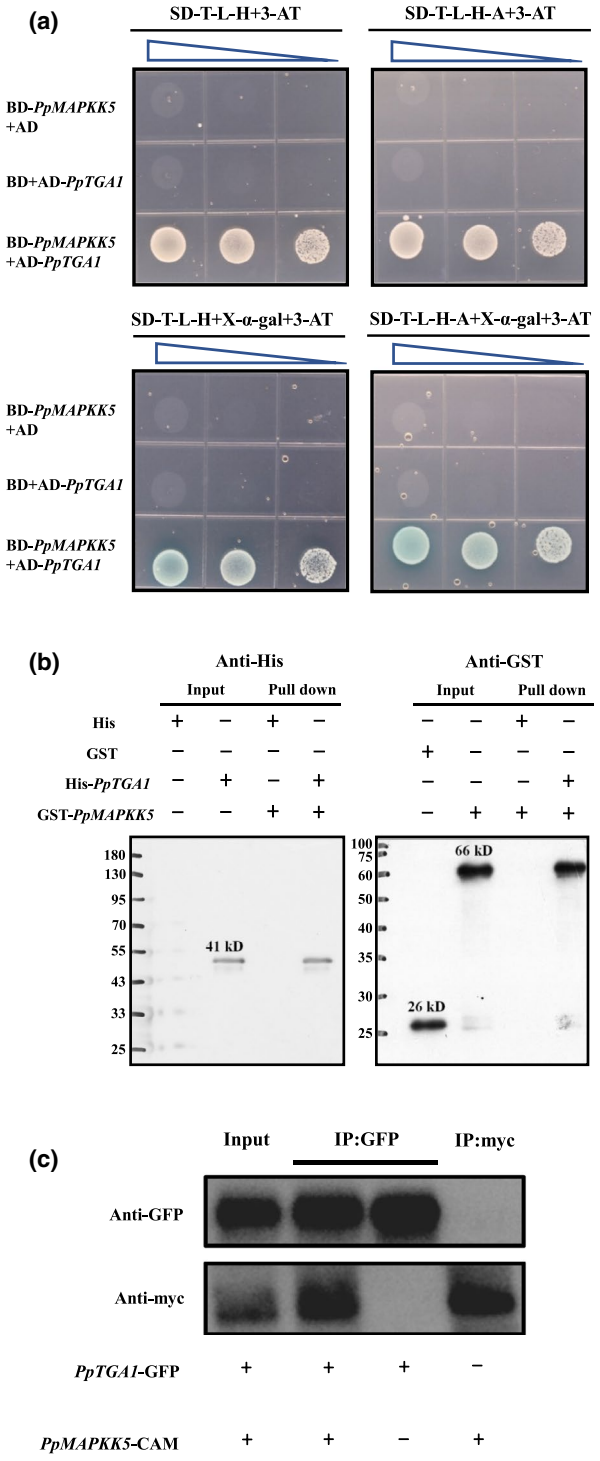

FIGURE 4 Confirmation of the interaction between PpTGA1 and PpMAPKK5. (a) Yeasts cultured on TDO (SD−T−L−H plate) or QDO (SD−T−L−H−A plate) with or without X-α-gal and 4 mM 3-AT. The triangles above Petri dishes indicate the amount of yeast cells determined by spectrophotometry at an optical density of 600 nm with 10-fold serial dilutions (from optical density of 1 to 0.01). (b) His-PpTGA1 recombinant protein preimmobilized on Ni-sepharose 6 Fast Flow and further incubated with GST-fused-PpMAPKK5 at 4°C for at least 8 h. The incubated resins were pelleted for immunoblot analysis with anti-His or anti-GST antibody. (c) Co-immunoprecipitation assay substantiated the PpTGA1 and PpMAPKK5 interaction in tobacco (*Nicotiana tabacum*)

2.5 | Confirmation of the PpTGA1/PpMAPKK5 interaction in vivo and in vitro

In the yeast two-hybrid (Y2H) system, the interaction between PpTGA1 and PpMAPKK5 stimulated the reporter genes *HIS3*, *ADE2*, and *MEL1*, as competent yeast AH109 cotransfected with BD-*PpMAPKK5* and AD-*PpTGA1* vectors presented colony clusters on synthetic dropout plates (SD/−Trp/−Leu/−His + 4 mM 3-AT and SD/−Trp/−Leu/−His/−Ade + 4 mM 3-AT) within 4–6 days, and these colonies turned blue on X-α-gal plates. In contrast, cells co-transformated with expected negative pairs (BD-*PpMAPKK5* + the empty pGADT7 vector and AD-*PpTGA1* + the empty pGBKT7 vector) barely grew on the TDO/QDO plates (Figure 4a). The western blot results from a His pull-down assay indicated that a specific binding band could not be detected in the absence of PpTGA1, revealing that PpTGA1 interacted with PpMAPKK5 in vitro (Figure 4b). The coimmunoprecipitation (Co-IP) assay confirmed the interaction between PpTGA1 and PpMAPKK5 in living plant cells (Figure 4c). PpTGA1 possesses five high-stringency phosphorylatible residues (Table S1). The amino acid motifs, including the kinase binding site group (Kin_bind), phosphoserine/threonine binding group (pST_bind), and basophilic serine/threonine kinase group (Baso_ST_kin), are located in the transcription factor TGA-like domain (IPR code IPR025422) of PpTGA1 but do not theoretically cover the basic leucine zipper domain (IPR code IPR004827; Figure S2).

2.6 | Nucleus-localized PpMAPKK5 acts cooperatively with PpTGA1 to activate the PR gene transcription

As presented in Figure 5a, the control construct harbouring the 35S::*GFP* cassette exhibited expression in both the cytoplasm and nucleus of stained onion peels; in contrast, the 35S::*PpMAPKK5-GFP* construct exhibited fusion protein expression that was observed exclusively in the nucleus, as highlighted by 4′,6-diamidino-2-phenylindole (DAPI) staining. The binding of PpTGA1 to the *PpPR1*, *PpPR2*, and *PpPR5* promoters in a yeast one-hybrid (Y1H) assay led to slight activation of the AbA reporter gene (Figure 5b). Moreover, when the *PpPR1*, *PpPR2*, or *PpPR5 Pro-LUC* reporter construct was coinfiltrated with *PpMAPKK5* and *PpTGA1*, the LUC/REN ratios were intensely induced and were much higher than those observed with *PpTGA1* alone (Figure 5c). These results indicate that PpMAPKK5 could apparently enhance the transactivation of PpTGA1 to the target *PR* genes.

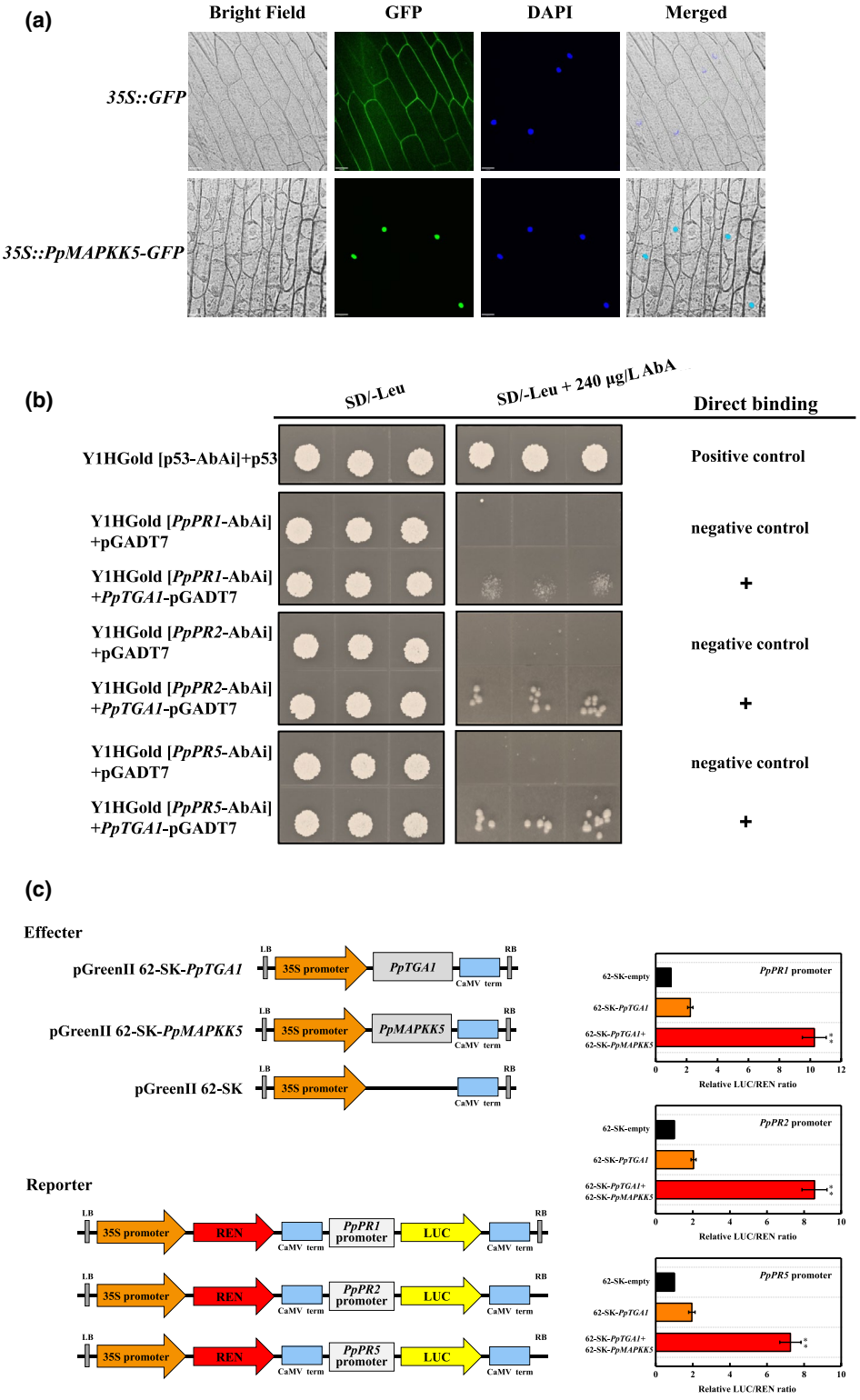

FIGURE 5 Nucleus-localized PpMAPKK5 acts synergistically with PpTGA1 to activate the expression of *PpPR* promoters. (a) Transient expression of the fusion protein (35S::*PpMAPKK5-GFP*) and positive control (35S::*GFP*) in onion peels was mediated by *Agrobacterium tumefaciens* infiltration. Green fluorescent protein (GFP) signals were captured using laser-scanning microscopy (Zeiss), and the white bar represents 70 μm in the horizontal direction. (b) Direct binding of PpTGA1 to *PpPR1*/*PpPR2*/*PpPR5* promoters was determined according to the ability of Y1H Gold [*PpPR1*/*PpPR2*/*PpPR5*-AbAi] + *PpTGA1*-pGADT7 to grow on SD/−Leu in the presence of 240 μg/L AbA. (c) Dual-luciferase reporter assay for the transactivation of PpTGA1 and PpMAPKK5 to the *PpPR1*, *PpPR2*, and *PpPR5* promoters. Activation is indicated by the ratio of LUC:REN; the empty plasmid combined with the promoter of *PpPR1*, *PpPR2* or *PpPR5* was set to 1 for the calibration of the ratio. Data represent the mean ± *SE* of nine independent repeats. ** indicates significant difference between samples ($p = 0.01$)

2.7 | Heterologous expression of *PpMAPKK5* elevates the resistance level to *R. stolonifer* and relieves cell death in *Arabidopsis*

PpMAPKK5 from *Prunus persica* is an orthologous gene of *Arabidopsis thaliana AtMAPKK5*; both cluster in group C (Figure S3). In this study, quantitative reverse transcription PCR (RT-qPCR) analysis indicated that the *PpMAPKK5* transcript profile was markedly higher in *A. thaliana PpMAPKK5*-overexpressing lines, especially in OE-6, OE-9, OE-12, and OE-18, compared with that in *A. thaliana* Col-0 wild-type (Figure 6a). Unexpectedly, the heterologous expression of *PpMAPKK5* retarded the growth of transgenic *Arabidopsis*, with the growth parameters in terms of dwarf leaves, leaf sizes, and biomasses being smaller than those of wild-type (WT) plants (Figure 6b,c). The mRNA levels of *AtNPR1* and *AtPR*s increased in the four *PpMAPKK5*-overexpressing lines (OE-6, OE-9, OE-12, and OE-18) at 3 and 6 days postinoculation (dpi) compared with those in WTs. There was an apparent accumulation of *AtNPR1* and *AtPR* transcripts after treating *PpMAPKK5*-overexpressing lines with BABA (Figure 6d). *R. stolonifer*-infected leaves were imaged after staining with lactophenol-trypan blue for the determination of pathogen growth and cell death-related activity. At 6 dpi, approximately half of the cells in WTs were blue-stained; in contrast, lesions and necrotic areas were significantly reduced in all transgenic lines (Figure 6e,f). The cell electrolyte leakage of *R. stolonifer*-infected transgenic leaves was obviously lower than that of WTs regardless of whether the WTs or overexpressing lines (OEs) were previously treated with BABA (Figure 6g). These results confirm that the overexpression of *PpMAPKK5* could contribute to the alleviation of cell damage and disease development.

2.8 | *AtMAPKK5* loss-of-function mutants showed decreased resistance to fungal pathogen

MAPKK5-knockout lines generated by the CRISPR/Cas9 system were collected to examine the role of MAPKK5 during fungal pathogen invasion. As presented in Figure 7a, the expression profile of *AtMAPKK5* in the knockout lines, including CRP-3, CRP-7, and CRP-11, drastically decreased by more than 91% compared with those in WTs. Conversely, CRP-3, CRP-7, and CRP-11 exhibited few alterations in growth phenotype, including leaf length, width, and biomass (Figure 7b,c). The CRISPR/Cas9-mediated *MAPKK5* knockout plants had similar expression patterns of a battery of *PR* genes, all of which slightly declined at 3 and 6 dpi (Figure 7d). Surprisingly, all knockout lines positively responded to BABA soil drench treatment, but the expression products of the *NPR1* and *PR* genes in these lines showed little significant difference from those of WT Col-0 (Figure 7d). Consistent with these observations, the disease symptoms and staining levels of the dot-inoculated knockout plants were slightly stronger than those of WT leaves (Figure 7e,f). As expected, the cell electrolyte leakage from knockout plants was also higher than that from WT plants, and plants treated with BABA were no exception (Figure 7g).

3 | DISCUSSION

Priming has an advantage over direct defence because of the balance of defence expression and its allocated metabolic costs (Buswell et al., 2018); however, there are only a few hypotheses regarding the underlying molecular mechanism. One hypothesis is that early elicitation by specific chemicals can prime and increase the accumulation of intracellular genes/proteins employed in the biosynthesis of various small signal molecules, including SA. Next, infection under high abiotic pressure stimulates latent signalling regulators, thus amplifying signal transduction cascades and providing augmented expression of host defence (Conrath et al., 2006; Mateo et al., 2006; Pastor et al., 2013). In this study, treatment of peaches with BABA alone significantly up-regulated a number of genes related to the ROS enzymatic scavenging system, the PPP for the NADPH supply, and the AsA-GSH cycle for the production of GSH and AsA during 72 hr of incubation (Figure 2). Moreover, BABA alone primed peaches to accumulate a higher SA level due to the induced transcription of a set of SA biosynthesis-related genes. In contrast, artificial fungal inoculation alone did not up-regulate the genes involved in redox regulation simultaneously, but the H_2O_2 burst was observed in the peaches challenged with *R. stolonifer* alone (Figure 3). Thus, it is probable that there are two distinct pathways associated with BABA- or pathogen-induced defence in harvested peach fruit. Specifically, BABA elicitation alone elevated the reductive status and possibly activated some critical redox-responsive regulators, while *R. stolonifer* infection only stimulated the ROS burst and defensive response. Such contrasting responses are reconciled by the redox homeostasis in an SA-dependent priming SAR in the BABA-treated and subsequently *R. stolonifer*-infected peaches, by which the generation of reductive substances primed the plant defence and an ROS burst magnified this defensive response. These data were also consistent with the finding of Tada et al. (2008), who highlighted the importance of redox homeostasis in priming expression in plants.

The modified intercellular redox conditions trigger the accumulation of a few pivotal regulators in their active conformation, which trains the plant innate immune system in a primed state (González-Bosch, 2018). NADPH oxidases, a kind of plasma membrane-bound RBOH protein, employ specific activity for the movement of NADPH-released electrons to oxygen and the generation of superoxide anions, which are subsequently dismutated to H_2O_2 by SOD (Kadota et al., 2015; Marino et al., 2012). *AtRBOHD*- or *AtRBOHF*-derived H_2O_2 accumulation has been determined to be a critical component of defence against biotic stress in *Arabidopsis* (Morales et al., 2016; Yao et al., 2017). Our work also provided evidence that an H_2O_2 burst could be closely connected with the enhanced transcript levels of *PpRBOHA* and *PpRBOHD* (the peach orthologous genes of *AtRBOHF* and *AtRBOHD*, respectively) and the potentiated activities of NADPH oxidases (Figures 3 and S4). However, the up-regulation of *PpRBOH* gene expression and the corresponding H_2O_2 burst occurred in only *R. stolonifer*-inoculated peaches, indicating a possible function of ROS in PTI or ETI. The BABA-primed peaches exhibited high *PpRBOHA* and *PpRBOHD* expression levels and H_2O_2

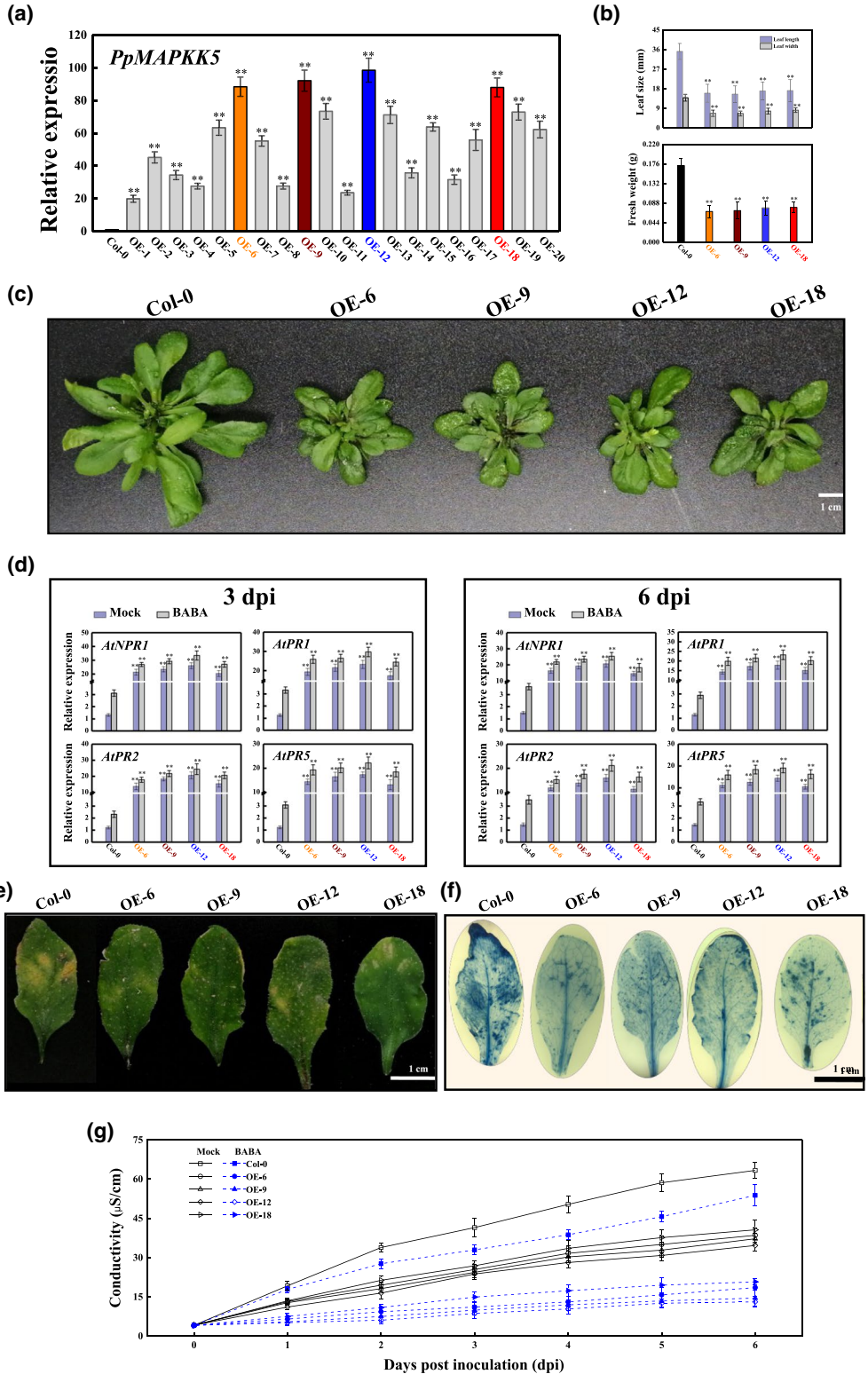

FIGURE 6 *PpMAPKK5* overexpression potentiates the expression of *PR*s and enhances *Arabidopsis* resistance to *Rhizopus stolonifer*. (a) *PpMAPKK5* transcription in 4-week-old wild-type (WT) and transgenic plants. Transcription was normalized against the value of the reference gene *AtActin2* and recorded as the mean ± *SE*. (b, c) The overexpression of *PpMAPKK5* hindered *Arabidopsis* growth, as indicated by the smaller leaf length and lower biomass in OE6, OE9, OE12, and OE18 as compared with those of WT plants (bar = 1 cm). (d) Quantitative reverse transcription PCR reflects the transcription of *NPR1* and *PR*s in WTs and OEs infected by *R. stolonifer* at 3 and 6 days postinoculation (dpi) with or without BABA treatment. **, significant ($p < 0.01$) difference between the WTs and OEs. (e) The disease symptoms of WT and *PpMAPKK5*-overexpressing *Arabidopsis* at 6 dpi. (f) *Arabidopsis* leaves of WTs and OEs were stained with trypan blue to reveal necrotic areas. (g) Electrolyte leakage levels of *Arabidopsis* leaves from WTs and OEs

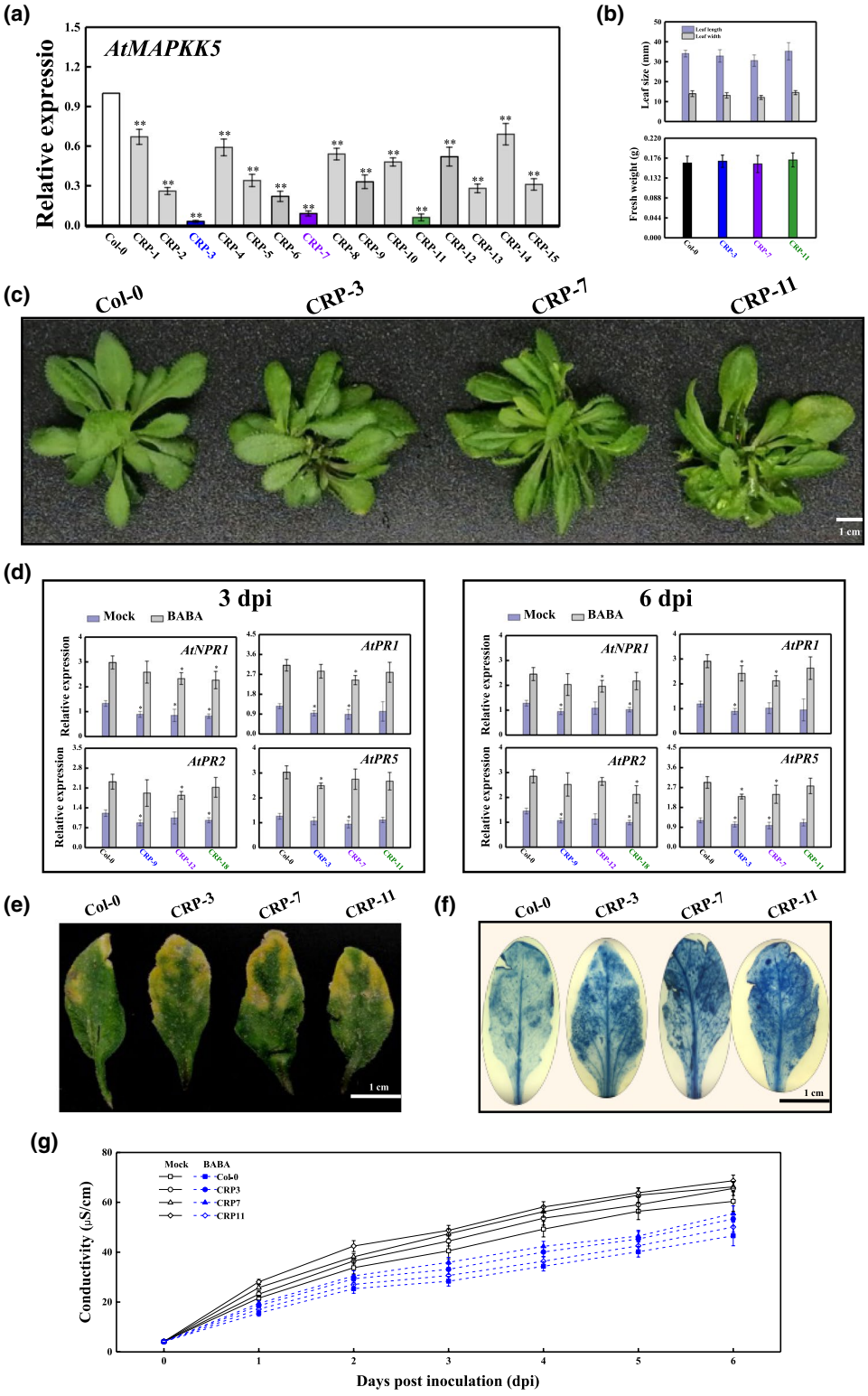

FIGURE 7 CRISPR/Cas9-mediated *MAPKK5* knockout lines showed slightly decreased resistance to the fungal pathogen *Rhizopus stolonifer*. (a) *AtMAPKK5* transcription in 4-week-old wild-type (WT) and knockout lines. (b, c) *MAPKK5* knockout did not change the speed of growth of *Arabidopsis*. (d) Transcription of NPR1 and *PRs* in WTs and knockout plants (CRP3, CRP7, and CRP11) after inoculation with *R. stolonifer* at 3 and 6 days postinoculation (dpi). (e) Disease symptoms of WTs and knockout plants at 6 dpi. (f) Necrotic areas in WTs and knockout plants were assessed by trypan blue staining at 6 dpi. (g) Electrolyte leakage levels of WTs and knockout plants infected with *R. stolonifer* at 6 dpi

peaks during the first 12 hr of incubation on infection with *R. stolonifer*, accompanied by enhanced resistance against the development of disease symptoms (Figures 1 and 3). Therefore, these results suggest that an RBOH-dependent ROS burst orchestrates fruit adaptation in the priming phase to augment the defensive response. On the other hand, MAPK cascades, known as the three-kinase pathway of MAPKKK-MAPKK-MAPK, are critical signalling components that can amplify and transduce various signals produced by receptor-like modules into a suitable intracellular response for combating stress or for development/reproduction requirements in eukaryotic plants (Gouda et al., 2020). Herein, we demonstrated that a set of *PpMAPKKK5* and *PpMAPKK5* genes were up-regulated in BABA-treated peaches (Figure 3c). Moreover, the induction of the *PpMAPKKK5*/*PpMAPKK5* genes in peaches elicited with BABA and subsequently inoculated with *R. stolonifer* was stronger than that observed after sole *R. stolonifer* challenge or BABA induction. Furthermore, this enhancement of *PpMAPKKK5*/*PpMAPKK5* genes by the combined treatment was consistent with the change in *PpRBOH* expression levels and H_2O_2 generation, indicating a direct connection between *PpMAPK* activation and *PpRBOH* expression for defence function. Similarly, PAMP-responsive MAPKs, including *Solanum lycopersicum* MAPK1/2 (Zhou et al., 2014), *Nicotiana benthamiana* MAPKKs (Adachi et al., 2016; Lee & Back, 2016), *N. benthamiana* WIPK and SIPK (Sharma et al., 2003; Zhang et al., 2012), *Oryza sativa* MAPK3/6 (Gupta et al., 2019), and MAPK3/4/6 of *Arabidopsis* (Beckers et al., 2009; Colcombet & Hirt, 2008; Liu et al., 2020), also acted as downstream sensors of early ROS/H_2O_2 rapid generation during signalling immune responses. Therefore, the RBOH-dependent H_2O_2 burst associated with pathogen recognition in primed peaches can be manifested as a hypersensitive messenger in response to disease stress that stimulates the MAPK cascade for the enhancement of signalling immunity.

A conserved MAPK cascade is composed of a three-linear signalling module, where the final downstream kinases of MAPKs have been proposed to phosphorylate targeted functional proteins and therefore transduce endogenous hormonal signals, promote gene transcription, and transfer metabolic flow towards defensive responses (Kishi-Kaboshi et al., 2010; Meng & Zhang, 2013). Interestingly, an interaction between MAPKKK1 and targeted WRKY53 provided a clue that MAPKKKs or MAPKKs can be released from redundant MAPK cascades for direct modification of downstream TFs (Miao et al., 2007). TGAs, representing a subclass of the basic leucine zipper (bZIP) TF family, contribute to interaction with NPR1 and form NPR1–TGA transcriptional complexes to activate downstream *PR* genes (Després et al., 2003; Zhang et al., 1999). Several bZIP TFs, including AtVIP1 from *Arabidopsis* and MaBZIP93 and MaBZIP74 from *Musa acuminata*, could act as the substrates of MAPKs and require phosphorylation modification for their regulatory functions (Djamei et al., 2007; Liang et al., 2020; Wu et al., 2019). The interaction between PpMAPKK5 and its probable substrate PpTGA1 could be observed not only in yeast cells but also in tobacco tissues (Figures 4 and S1). Meanwhile, the His pull-down results confirmed the formation of the PpMAPKK5-PpTGA1 complex in vitro (Figure 4). PpTGA1, containing several phosphorylation motifs, including Kin_bind, pST_bind, and Baso_ST_kin, could be the target of pathogen-responsive MAPKK5 (Figure S2 and Table S1). These data suggested that PpMAPKK5 interacts with PpTGA1 through probable phosphorylation modification. In particular, neither PpMAPKKKs nor PpMAPKs interacted with PpTGA1 in the Y2H library screen (Figure S1). Thus, we deduced that the direct signalling of PpMAPKK5 to PpTGA1 could bypass the normal MAPK cascade for possible posttranslational phosphorylation. In the Y1H system and DLR assay, PpTGA1 was identified as a DNA-binding protein that served as a transcriptional activator of *PpPR* genes; moreover, PpMAPKK5 could confer an increased transactivation capacity to PpTGA1 (Figure 5). Additionally, PpMAPKK5 was stably located in the nucleus, which was in accordance with the nuclear localization of PpTGA1 after redox-dependent translocation as described previously (Li et al., 2020b). The same nuclear localization shared by PpMAPKK5 and its downstream target PpTGA1 implied that the interaction occurred predominantly in nuclei and strengthened NPR1–TGA1 transactivation. As a result, PpMAPKK5 can be recognized as a candidate signalling enzyme that mediates the TGA1-dependent priming defence in peach fruit. The overexpression of *PpMAPKK5* in transgenic *Arabidopsis* caused constitutive transcription of SA-responsive *PR* genes and lowered their sensitivity to *R. stolonifer*, whereas *Arabidopsis MAPKK5* loss-of-function mutants displayed compromised expression of *PR* genes (Figures 6 and 7). The results further support the conclusion that the SAR defence in peach fruit could result from *PpMAPKK5* activation at least in part. However, BABA elicitation dramatically induced *PR* gene expression in the *MAPKK5* knockout lines (Figure 7d), which raises the question of whether BABA stimulates the SAR reaction by another branched defence pathway.

Based on the molecular and genetic trials conducted in the present study, we suggest that the typical BABA-mediated priming resistance of peach fruit involves the primed intracellular redox homeostasis associated with intracellular signal transudation and subsequent amplification of the signalling events to activate a more rapid and stronger defence on pathogen invasion (Figure 8). This priming of host–pathogen interaction processes can be attributed to a TGA1-dependent SAR reaction, in which the direct interaction of PpTGA1 and PpMAPKK5 may increase the DNA-binding activity of PpTGA1 for *PR* gene transcription. A few publications and this study have provided possible molecular mechanisms involved in the priming defence in horticultural crops, but the translation of defence priming to practical use will be a crucial issue for future research.

4 | EXPERIMENTAL PROCEDURES

4.1 | Plant and pathogen materials

P. persica 'Baifeng' peaches were procured and hand-picked from a standard peach orchard located in Tongnan District, Chongqing City in China. These peaches were transferred to our laboratory under

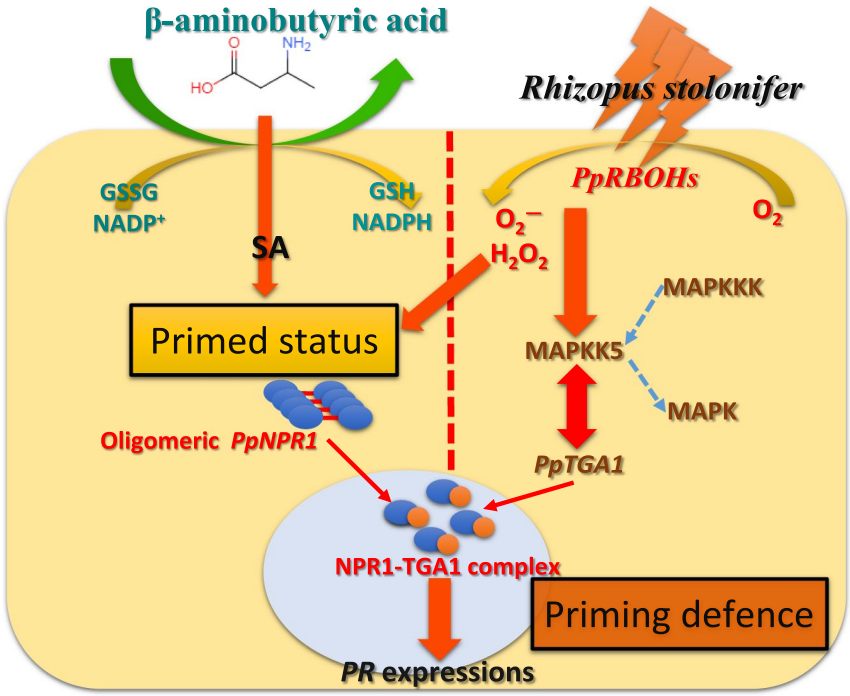

FIGURE 8 A simplified model of redox homeostasis and shortcut interaction between TGA1 and MAPKK5 involved in BABA-induced priming defence in postharvest peach fruit

chilled conditions and were individually distributed on an experimental console at 20°C until used for BABA treatment and pathogen inoculation.

The Columbia-0 (Col-0) ecotype of *A. thaliana* was the genetic background for the transgenic and mutant plants presented in our current work. Col-0 WT seeds were surface-sterilized with sodium hypochlorite and cold-stratified for approximately 3 days at 4°C before being sown in soil and cultured in an illumination incubator (SPT-P500B, Darth Carter Co.) under a long-day (LD) photoperiod (60%–70% RH, 2500–3000 lx, 22°C under 14 h/10 h light/dark cycles) for more than 4 weeks. In addition to *Arabidopsis*, tobacco (*Nicotiana tabacum*) employed for *Agrobacterium tumefaciens*-mediated transient transformation was cultivated in an illumination incubator with the same LD conditions for 5–9 weeks in accordance with our previously described methodology (Li et al., 2020a).

R. stolonifer was isolated and identified according to our recent works (Li et al., 2020a). The *R. stolonifer* mycelia were incubated on potato dextrose agar (PDA) for 3–4 days (26°C) and rinsed thoroughly with sterile water with 0.5% (vol/vol) Tween 80 for the preparation of *R. stolonifer* spore suspensions, which were diluted to 10^5 spores/ml (for the inoculation treatment of peach fruit) and 2×10^5 spores/ml (for the detection of pathogen resistance in transgenic and mutant *Arabidopsis*) using a Neubauer chamber.

4.2 | BABA treatment and spore inoculation

Intact peaches with identical size and maturity without visible mechanical damage were surface-sterilized with 75% (vol/vol) alcohol, air-dried for more than 3 h at 20°C, and further partitioned into four groups of 360 peaches each. Two uniform holes were punched per peach by perforating 3 mm deep and 3 mm wide wounds around the centre of each peach at two symmetrical sites with a sterile, dissecting needle. The specific concentration of BABA (50 mM, purity of ≥99%; Sigma Co.) was chosen on the basis of our previous studies, which demonstrated that 50 mM BABA could effectively elicit a priming defence in peaches (Li et al., 2020a). The wounds of each group were injected with distilled water (control), the BABA solution (BABA elicitation), the spore suspensions of *R. stolonifer* (*R. stolonifer* inoculation), or BABA followed by *R. stolonifer* inoculation (BABA + inoculation; Li et al., 2020a, 2020b). After treatment, all peaches were arrayed on an experimental console for approximately 6 h, sealed in polyethylene boxes (60 μm thickness), and placed in incubators for 72 h at 20 ± 1°C with 80%–90% RH. Finally, 30–50 g tissue from the uninfected sarcocarp (2–3 mm in length away from the infected area) of 60 peaches in each group was sampled with a sterile scalpel before incubation (0 h) and at 12 h intervals during 72 h of incubation at 20°C. Fruit pulps sampled from each individual were then frozen in liquid N_2 and stored at −80°C until further analysis. Each treatment comprised three replicates with a completely randomized design and the entire experiment was executed twice with similar results.

4.3 | Evaluation of disease development

The peach was recorded as diseased when the width of the inoculated area exceeded 3 mm. The disease incidence was calculated by determining the proportion of decaying peaches. Disease development, including the lesion diameter and disease incidence, in each triplicate sample was observed sequentially for 72 h at 24 h intervals.

4.4 | Measurement of NADPH oxidase activity

Plasma membrane vesicles were isolated from peaches with two-phase partitioning according to a previously described method (Morré & Morré, 2000). The NADPH-dependent O_2^--generating activity in membrane vesicles was measured by the reduction of XTT by O_2^- (adapted from Sagi & Fluhr, 2001; Zhang et al., 2009). NADPH oxidase activity was expressed as O_2^- nmol/min/g fresh weight (FW).

4.5 | Determination of H_2O_2 content

The titanium (IV) method described previously by Patterson et al. (1984) was conducted for measurement of endogenous H_2O_2 content, which was presented as μmol/kg FW.

4.6 | RNA isolation and RT-qPCR

Total RNA was isolated using the RNAprep Pure Kit for plants (Tiangen) from powdered frozen tissues (5 g) and single-stranded cDNA was synthesized by aliquots (1 μg) of RNA using a PrimeScript RT Reagent Kit (Takara). Quantitative PCR (qPCR) was performed with SYBR Green in triplicate on a 7500 FAST Real-Time PCR system (Applied Biosystems). Gene-specific primer pairs (listed in Table S2) were designed using Primer3 software available in the NCBI database with expected amplicon lengths between 90 and 150 bp to minimize the impact of the RNA and ensure optimal polymerization efficiency. The qPCR mixture and the thermal cycling parameters were prepared and set according to our previous study (Li et al., 2021). The gene expression levels were calculated using the $2^{-\Delta\Delta Ct}$ method (Livak & Schmittgen, 2001). For normalization of the qPCR results, peach *TEF2* (adapted from Tong et al., 2009) or *Arabidopsis Actin2* genes were used as internal standards.

4.7 | Construction and evaluation of peach fruit cDNA library

Total RNA from BABA-pretreated plus *R. stolonifer*-inoculated pulp at 12 hpi was extracted using the TRIzol method (Invitrogen). One microgram of total RNA was reverse-transcribed to dscDNA with a SMART cDNA Library Construction Kit (Clontech). dscDNA was purified using VAHTS DNA Clean Beads (Vazyme) and further recombined into the linearized pGADT7 vector, and the recombinant product was transformed into *E. coli* DH5α electroporation-competent cells to generate the Y2H library. The constructed cDNA library was subjected to a plating assay to determine the optimal titre (cfu/ml, Gao et al., 2015). For confirmation of the cDNA inserts, the 24 randomly picked cDNA clones were subjected to colony PCR (initial denaturation at 95°C for 3 min; followed by 25 cycles of 95°C for 15 s, 55°C for 15 s and 72°C for 1 min; and then extension for 5 min at 72°C). Further electrophoresis-based detection revealed that most of the inserts appeared as a single band and ranged from 0.1 to 1.5 kb in size (Figure S5).

4.8 | Bait plasmid construction and the determination of its self-activation activity

The synthesized *PpTGA1* was cloned into the *Bam*HI-*Sma*I sites of the yeast expression vector pGBKT7 to form the bait plasmid (pGBKT7-*PpTGA1*). The competent cells of *Saccharomyces cerevisiae* AH109 were transformed with pGBKT7-*PpTGA1* using the lithium acetate method, and the transformants were plated on SD/−Trp medium. Single colonies were selected and confirmed using Matchmaker Insert Check PCR Mix 2 (Takara). The autotranscriptional activation of the positive pGBKT7-*PpTGA1* colonies was tested on SD/−Trp/−His (double dropout, DDO), SD/−Trp/−His/−Ade (triple dropout, TDO), and TDO + X-α-gal plates with or without the serial addition of 3-amino-1,2,4-triazole (3-AT) at 29°C.

4.9 | Screening of the cDNAs for *PpTGA1*

The bait strain harbouring pGBKT7-*PpTGA1-2* was transformed with 25 μg library plasmid in a yeast-mating procedure. The cotransformants were plated on SD/−Trp/−Leu/−His plates containing 10 or 20 mM 3-AT and incubated at 29°C for 5–9 days (Figure S1). All single colonies were then transferred twice to new TDO (SD/−Trp/−Leu/−His plate) supplemented with 10 or 20 mM 3-AT for double selection. The pGADT7-cDNA plasmids encoding the interacting proteins of PpTGA1 were extracted from shake-cultured (in SD/−Trp/−Leu/−His liquid medium, 29°C/225 rpm) colonies through a yeast plasmid isolation kit (Omega), transformed into *E. coli* DH5α cells and further subjected to colony PCR, DNA sequencing, and BLAST analysis before verification on synthetic dropout plates.

4.10 | Y2H assay

Y2H analysis was further performed by employing the Matchmaker GAL4-based Y2H system (Clontech) to examine the interaction between the identified PpMAPKK5 and PpTGA1. The coding regions of *PpMAPKK5* and *PpTGA1* were fused to the pGBKT7 and pGADT7 vectors to construct the bait (BD-*PpMAPKK5*) and prey (AD-*PpTGA1*) expression vectors, respectively. The two constructs were inserted into *S. cerevisiae* AH109 cells and then plated on synthetic dropout media with the addition of X-α-gal (40 mg/L) as previously described (Wang et al., 2021).

4.11 | Pull-down assay

The synthesized *PpMAPKK5* or *PpTGA1* was cloned into the pGEX-4T-1 or pET-28a vector to produce the corresponding glutathione

S-transferase (GST)- or His-tagged proteins, respectively. Then, the two fusion proteins were expressed in *E. coli* BL21 (DE3) and protein expression was induced with 0.1 mM isopropyl β-D-galactopyranoside (IPTG) for 16 h at 20°C. Bacteria expressing the GST fusion protein (PpMAPKK5) were lysed through sonication and purified with glutathione agarose (Thermo Fisher Scientific) based on the instructions. For the pull-down assay, the recombinant His-PpTGA1 was immobilized with Ni-Sepharose beads (Ni-Sepharose 6 Fast Flow; GE Healthcare) for 2 h at 4°C. Subsequently, the recombinant GST-PpMAPKK5 or GST was incubated with prewashed beads for more than 8 h at 4°C before being washed with ice-cold phosphate-buffered saline (PBS). After boiling in 2 × Laemmli buffer, 6 μl of the pulled-down proteins was examined by western blotting using anti-GST antibodies (TransGen Biotech Co., Ltd), and His +recombinant GST-PpMAPKK5 served as the negative control.

4.12 | Co-IP assay

A Co-IP assay was performed as previously described (Wang et al., 2021). The full-length coding sequences of *PpMAPKK5* and *PpTGA1* were introduced into pCAMBIA35s-4 × myc and pBinGFP2, respectively. The recombinant proteins (PpMAPKK5-CAM harbouring myc-label and PpTGA1-GFP harbouring GFP-label) were transformed into *Agrobacterium tumefaciens* GV3101 and infiltrated into 8-week-old tobacco leaves. The infected leaves were cultivated for an additional 48 h under LD conditions. The isolated leaf proteins were either exposed directly to 12% SDS-PAGE for western immunoblotting analysis or immunoprecipitated overnight with horseradish peroxidase (HRP) anti-GFP antibody (1:2,000; Invitrogen) or HRP anti-myc antibody (1:2,000; Invitrogen). The immune complexes were collected using protein A/G-agarose (PA/G, Santa Cruz Biotechnology) and washed eight times with commercial wash buffer. For immunoblotting, the isolated proteins or pellets were suspended in 1 × SDS-PAGE loading buffer, separated on SDS-polyacrylamide gels and transferred to nitrocellulose membranes. The membranes were immunoblotted with anti-GFP antibody or anti-myc antibody and visualized using the ECL-Plus western blotting system (GE-Healthcare).

4.13 | Subcellular localization of *PpMAPKK5*

PCR-amplified *PpMAPKK5* was inserted into the binary expression vector pCAMBIA1301-35S-*GFP* at the 5′-terminus of the green fluorescent protein (GFP) driven by the 35S promoter of cauliflower mosaic virus (CaMV). The fusion protein vector of 35S::*PpMAPKK5-GFP* and the empty vector of 35S::*GFP* were introduced into *A. tumefaciens* EHA105 and further transformed into onion bulb epidermis cells as described previously (Li et al., 2021). After 3 days of cultivation on Murashige & Skoog (MS) medium in the dark (26°C), onion bulbs were stained with 20 μg/ml DAPI nuclear dye (Sigma). The fluorescence signals of the stained onion peels were visualized by fluorescence microscopy (LSM 510; Zeiss) with excitation wavelengths at 488 nm for the GFP signal and 405 nm for the DAPI fluorescence at 3 h after staining. Herein, 35S::*GFP* served as the positive control.

4.14 | Y1H assay

The Y1H assay was conducted using the Matchmaker gold Y1H system (Clontech). Three copies of the TGACG-motif *cis*-acting elements and their adjacent nucleotides (approximately 50 bp) were synthesized on the basis of the promoter fragments of *PpPRs* (Data S1) and ligated into the pAbAi vector. Then, *PpPR1*-AbAi, *PpPR2*-AbAi, *PpPR5*-AbAi, and p53-AbAi were linearized by *Bbs*I and transformed into the Y1H Gold strain. The construction of recombinant *PpTGA1*-pGADT7, determination of the minimal inhibitory concentration (MIC) of AbA and detection of direct binding among PpTGA1, *PpPR1*, *PpPR2*, and *PpPR5* were performed according to our previous study (Wang et al., 2021).

4.15 | Dual-luciferase reporter assay

Transactivation of the *PpPR1*, *PpPR2*, and *PpPR5* promoters by PpTGA1 and PpMAPKK5 was determined according to a dual-luciferase system, in which the coding sequence fragments of *PpTGA1* and *PpMAPKK5* in BABA plus *R. stolonifer*-inoculated peaches were introduced into the pGreenII 62-SK vector to serve as effectors (pGreenII 62-SK-*PpTGA1*/*PpMAPKK5*), and the *PpPR1*, *PpPR2*, and *PpPR5* promoters were inserted into the pGreenII 0800-LUC vector to construct reporters (pGreenII 0800-LUC-*PpPR1*/*PpPR2*/*PpPR5*). The effectors and reporters were then transformed into *A. tumefaciens* GV3101. The GV3101 cells harbouring effectors were mixed in equal proportions and further blended with each reporter and infiltrated into 5- to 9-week-old tobacco plants (abaxial leaf surfaces). The binding activities of PpTGA1 and PpMAPKK5 to the *PpPR* promoters were measured as described by Shan et al. (2016) and reported as the LUC:REN ratio. At least nine independent repeats were performed for each pair.

4.16 | Transgenic *Arabidopsis* overexpressing *P. persica MAPKK5*

The entire coding region (1062 bp) of *PpMAPKK5* amplified from peach cDNA was fused downstream of the enhanced CaMV 35S promoter in the plant overexpression vector pCAMBIA 1305.1 to obtain the heterologous overexpression plasmid 35S::*PpMAPKK5*. *Arabidopsis* plants were immersed in *A. tumefaciens* GV3101 cells harbouring the 35S::*PpMAPKK5* construct with the floral dip method (Clough & Bent, 1998). The T_1 seeds were harvested and sterilized in 2% sodium hypochlorite for approximately 10 min before stratification at 4°C (3 days) and further germinated on

half-strength MS medium (½MS; Murashige & Skoog, 1962) supplemented with kanamycin (Kan, 50 mg/L) for approximately 7 days. The Kan-resistant seedlings were then sown in 11-cm germination pots containing a prepared soil mixture of vermiculite and perlite in a 2:1 ratio and placed in a chamber under LD conditions. Homozygous transgenic plants in the T_3 generation were prepared for follow-up experiments.

4.17 | Generation of *MAPKK5* knockout mutants using the CRISPR-Cas9 system

The specific guide RNA (sgRNA) cassettes on the strand of targeted *AtMAPKK5* were chosen according to GC abundance and sequences corresponding to the protospacer adjacent motif (PAM) sites (set as 'NGG'), and their off-target effects were confirmed using the web server CRISPR-P (http://crispr.hzau.edu.cn/CRISPR2/). The annealed sgRNA cassettes were ligated into the *Bsa*I-digested M2CRISPR binary vector to generate the CRISPR/Cas9 vector of U26 promoter-driven T1 sgRNA and U29 promoter-driven T2 sgRNA (the vector construction diagram is shown in Figure S6). Details regarding the primers used for the generation of *MAPKK5* loss-of-function mutants are listed in Table S2. The CRISPR/Cas9 construct was transformed into *Arabidopsis* using *A. tumefaciens*-mediated transformation. Then, T_1 generation transformants were selected on MS medium with hygromycin phosphtotransferase (HYG, 50 mg/L). Genomic DNA was isolated from 4-week-old knockout lines, followed by PCR amplification with KOD FX (Toyobo Co. Ltd) using the gene-specific primers listed in Table S2 to detect mutational events. After the verification of homozygous mutants, T_3 mutant seedlings were harvested.

4.18 | Inoculation of *Arabidopsis* with *R. stolonifer* after drenching the plants with BABA

After soil drench treatment with 30 μg/mL BABA according to the previous method of Zimmerli et al. (2001), 4-week-old soil-grown T_3 transgenic and WT *Arabidopsis* Col-0 plants were dot-inoculated with 10-μl droplets of *R. stolonifer* conidial suspensions (2×10^5 conidia/ml) at fixed and symmetrical positions on leaf midveins as described by Xiao and Chye (2011). Then, detached leaves were prepared for the detection of resistance-related gene transcription at 3-day intervals and leaves at 6 dpi were prepared for morphological observations.

4.19 | Trypan blue staining

Pathogen-infected *Arabidopsis* leaves at 6 dpi were immersed in boiling trypan blue staining solution as described previously by Cai et al. (2020) and further soaked in chloral hydrate solution (1.25 g/ml) for approximately 1.5 days and photographed using binocular stereomicroscopy (EZ4D; Leica).

4.20 | Electrolyte leakage measurement

Leaf discs (8 mm diameter) of *R. stolonifer*-infiltrated leaves from WTs, OEs, and knockout plants were washed twice with 50 ml double-deionized water and then floated on double-deionized water as described by Mackey et al. (2002). The water conductivity was measured by a conductivity meter (MIK-TDS210-B).

4.21 | Data analysis

All data were separated with *t* test and one-way analysis of variance (Tukey's test) using the SPSS package program for Windows v. 13.0 (SPSS Inc.); values were shown as the mean ± *SE* of the six replicates from two independent experiments. Different letters and asterisks indicate significant differences between treatments at $p = 0.05$ or 0.01.

ACKNOWLEDGEMENTS

The research was funded by the National Natural Science Foundation of China (nos. 31671913 and 31672209), the Natural Science Foundation of Ningbo City (no. 2018A610224), and the Funds for Innovative Research Groups of University in Chongqing City (CXQT21036). We thank Yunxia Liao, Si Chen, and Dongzhi Wu for sample preparation in the past 5 years. We also especially thank Prof. Wei Deng (Chongqing University), Dr. Zhongqi Fan (Fujian A&F University) and Dr. Leigang Zhang (JAAS) for their helpful advice or scientific editing.

CONFLICT OF INTEREST

The authors declare that there is no conflict of interest.

DATA AVAILABILITY STATEMENT

The data that supports the findings of this study are available from the corresponding author upon reasonable request.

ORCID

Chunhong Li https://orcid.org/0000-0002-7133-0301
Kaituo Wang https://orcid.org/0000-0002-3534-2903

REFERENCES

Adachi, H., Ishihama, N., Nakano, T., Yoshioka, M. & Yoshioka, H. (2016) *Nicotiana benthamiana* MAPK-WRKY pathway confers resistance to a necrotrophic pathogen *Botrytis cinerea*. *Plant Signaling & Behavior*, 11, e1183085.

Baggio, J., Hau, B. & Amorim, L. (2017) Spatiotemporal analyses of Rhizopus rot progress in peach fruit inoculated with *Rhizopus stolonifer*. *Plant Pathology*, 66, 1452–1462.

Beckers, G.J.M., Jaskiewicz, M., Liu, Y., Underwood, W.R., He, S.Y., Zhang, S.Q. et al. (2009) Mitogen-activated protein kinases 3 and 6 are required for full priming of stress responses in *Arabidopsis thaliana*. *The Plant Cell*, 21, 944–953.

Buswell, W., Schwarzenbacher, R.E., Luna, E., Sellwood, M., Chen, B., Flors, V. et al. (2018) Chemical priming of immunity without costs to plant growth. *New Phytologist*, 218, 1205–1216.

Cai, J.H., Chen, T., Wang, Y., Qin, G.Z. & Tian, S.P. (2020) *SlREM1* triggers cell death by activating an oxidative burst and other regulators. *Plant Physiology*, 183, 717–732.

Canet, J.V., Dobón, A., Roig, A. & Tornero, P. (2010) Structure–function analysis of *npr1* alleles in *Arabidopsis* reveals a role for its paralogs in the perception of salicylic acid. *Plant, Cell & Environment*, 33, 1911–1922.

Clough, S.J. & Bent, A.F. (1998) Floral dip: a simplified method for *Agrobacterium*-mediated transformation of *Arabidopsis thaliana*. *The Plant Journal*, 16, 735–743.

Cohen, Y., Vaknin, M. & Mauch-Mani, B. (2016) BABA-induced resistance: milestones along a 55-year journey. *Phytoparasitica*, 44, 513–538.

Colcombet, J. & Hirt, H. (2008) *Arabidopsis* MAPKs: a complex signalling network involved in multiple biological processes. *Biochemical Journal*, 413, 217–226.

Coll, N.S., Epple, P. & Dangl, J.L. (2011) Programmed cell death in the plant immune system. *Cell Death and Differentiation*, 18, 1247–1256.

Conrath, U., Beckers, G.J.M., Flors, V., García-Agustín, P., Jakab, G., Mauch, F. et al. (2006) Priming: getting ready for battle. *Molecular Plant-Microbe Interactions*, 19, 1062–1071.

Després, C., Chubak, C., Rochon, A., Clark, R., Bethune, T., Desveaux, D. et al. (2003) The *Arabidopsis* NPR1 disease resistance protein is a novel cofactor that confers redox regulation of DNA binding activity to the basic domain/leucine zipper transcription factor TGA1. *The Plant Cell*, 15, 2181–2191.

Djamei, A., Pitzschke, A., Nakagami, H., Rajh, I. & Hirt, H. (2007) Trojan horse strategy in *Agrobacterium* transformation: abusing MAPK defense signaling. *Science*, 318, 453–456.

Dong, X.N. (2004) NPR1, all things considered. *Current Opinion in Plant Biology*, 7, 547–552.

Gao, J.X., Jing, J., Yu, C.J. & Chen, J. (2015) Construction of a high-quality yeast two-hybrid library and its application in identification of interacting proteins with Brn1 in *Curvularia lunata*. *Plant Pathology Journal*, 31, 108–114.

Glazebrook, J. (2005) Contrasting mechanisms of defense against biotrophic and necrotrophic pathogens. *Annual Review of Phytopathology*, 43, 205–227.

González-Bosch, C. (2018) Priming plant resistance by activation of redox-sensitive genes. *Free Radical Biology & Medicine*, 122, 171–180.

Gouda, M.H.B., Zhang, C.J., Wang, J.H., Peng, S.J., Chen, Y.R., Luo, H.B. et al. (2020) ROS and MAPK cascades in the post-harvest senescence of horticultural products. *Journal of Proteomics & Bioinformatics*, 13, 1–7.

Gupta, R., Min, C.W., Kim, Y.J. & Kim, S.T. (2019) Identification of Msp1-induced signaling components in rice leaves by integrated proteomic and phosphoproteomic analysis. *International Journal of Molecular Sciences*, 20, 4135–4151.

Gust, A.A., Biswas, R., Lenz, H.D., Rauhut, T., Ranf, S., Kemmerling, B. et al. (2007) Bacteria-derived peptidoglycans constitute pathogen-associated molecular patterns triggering innate immunity in *Arabidopsis*. *Journal of Biological Chemistry*, 282, 32338–32348.

Jonak, C., Okresz, L., Bogre, L. & Hirt, H. (2002) Complexity, cross talk and integration of plant MAP kinase signaling. *Current Opinion in Plant Biology*, 5, 415–424.

Kadota, Y., Shirasu, K. & Zipfel, C. (2015) Regulation of the NADPH oxidase RBOHD during plant immunity. *Plant and Cell Physiology*, 56, 1472–1480.

Kishi-Kaboshi, M., Okada, K., Kurimoto, L., Murakami, S., Umezawa, T., Shibuya, N. et al. (2010) A rice fungal MAMP responsive MAPK cascade regulates metabolic flow to antimicrobial metabolite synthesis. *The Plant Journal*, 63, 599–612.

Kohler, A., Schwindling, S. & Conrath, U. (2002) Benzothiadiazole-induced priming for potentiated responses to pathogen infection, wounding, and infiltration of water into leaves requires the *NPR1/NIM1* gene in *Arabidopsis*. *Plant Physiology*, 128, 1046–1056.

Kwon, J.H. & Lee, C.J. (2006) *Rhizopus* soft rot on pear (*Pyrus serotina*) caused by *Rhizopus stolonifer* in Korea. *Mycobiology*, 34, 151–153.

Lee, H.Y. & Back, K. (2016) Mitogen-activated protein kinase pathways are required for melatonin-mediated defense responses in plants. *Journal of Pineal Research*, 60, 327–335.

Li, C., Cao, S., Wang, K., Lei, C., Ji, N., Xu, F. et al. (2021) Heat shock protein HSP24 is involved in the BABA-induced resistance to fungal pathogen in postharvest grapes underlying an NPR1-dependent manner. *Frontiers in Plant Science*, 12, 646147.

Li, C., Wang, J., Ji, N., Lei, C., Zhou, D., Zheng, Y. et al. (2020a) *PpHOS1*, a RING E3 ubiquitin ligase, interacts with *PpWRKY22* in the BABA-induced priming defense of peach fruit against *Rhizopus stolonifer*. *Postharvest Biology and Technology*, 159, 111029–111037.

Li, C.H., Wang, K.T. & Zheng, Y.H. (2020b) Redox status regulates subcelluar localization of *PpTGA1* associated with a BABA-induced priming defence against *Rhizopus* rot in peach fruit. *Molecular Biology Reports*, 47, 6657–6668.

Li, C.H., Wang, K.T., Lei, C.Y. & Zheng, Y.H. (2020c) Translocation of *PpNPR1* is required for β-aminobutyric acid-triggered resistance against *Rhizopus stolonifer* in peach fruit. *Scientia Horticulturae*, 272, 1–10.

Liang, S.-M., Chen, S.-C., Liu, Z.-L., Shan, W., Chen, J.-Y., Lu, W.-J. et al. (2020) *MabZIP74* interacts with *MaMAPK11-3* to regulate the transcription of *MaACO1/4* during banana fruit ripening. *Postharvest Biology and Technology*, 169, 111293–111302.

Liu, Y., Yan, J., Qin, Q., Zhang, J., Chen, Y., Zhao, L. et al. (2020) Type 1 protein phosphatases (TOPPs) contribute to the plant defense response in Arabidopsis. *Journal of Integrative Plant Biology*, 62, 360–377.

Livak, K.J. & Schmittgen, T.D. (2001) Analysis of relative gene expression data using real-time quantitative PCR and the $2^{-\Delta\Delta Ct}$ method. *Methods*, 25, 402–408.

Mackey, D., Holt, B.F. III, Wiig, A. & Dangl, J.L. (2002) RIN4 interacts with *Pseudomonas syringae* type III effector molecules and is required for *RPM1*-mediated resistance in *Arabidopsis*. *Cell*, 108, 743–754.

Marino, D., Dunand, C., Puppo, A. & Pauly, N. (2012) A burst of plant NADPH oxidases. *Trends in Plant Science*, 17, 9–15.

Mateo, A., Funck, D., Mühlenbock, P., Kular, B., Mullineaux, P.M. & Karpinski, S. (2006) Controlled levels of salicylic acid are required for optimal photosynthesis and redox homeostasis. *Journal of Experimental Botany*, 57, 1795–1807.

Meng, X. & Zhang, S. (2013) MAPK cascades in plant disease resistance signaling. *Annual Review of Phytopathology*, 51, 245–266.

Miao, Y., Laun, T.M., Smykowski, A. & Zentgraf, U. (2007) Arabidopsis MEKK1 can take a short cut: it can directly interact with senescence-related WRKY53 transcription factor on the protein level and can bind to its promoter. *Plant Molecular Biology*, 65, 63–76.

Morales, J., Kadota, Y., Zipfel, C., Molina, A. & Torres, M.A. (2016) The Arabidopsis NADPH oxidases RbohD and RbohF display differential expression patterns and contributions during plant immunity. *Journal of Experimental Botany*, 67, 1663–1676.

Morré, D.J. & Morré, D.M. (2000) Applications of aqueous two-phase partition to isolation of membranes from plants: a periodic NADH oxidase activity as a marker for right side-out plasma membrane vesicles. *Journal of Chromatography B: Biomedical Sciences and Applications*, 743, 369–376.

Murashige, T. & Skoog, F. (1962) A revised medium for rapid growth and bioassays with tobacco tissue cultures. *Physiologia Plantarum*, 15, 473–497.

Mutalik, V.K. & Venkatesh, K.V. (2006) Effect of the MAPK cascade structure, nuclear translocation and regulation of transcription factors on gene expression. *Biosystems*, 85, 144–157.

Pastor, V., Luna, E., Ton, J., Cerezo, M., García-Agustín, P. & Flors, V. (2013) Fine tuning of reactive oxygen species homeostasis regulates primed immune responses in *Arabidopsis*. *Molecular Plant-Microbe Interactions*, 26, 1334–1344.

Patterson, B.D., MacRae, E.A. & Ferguson, I.B. (1984) Estimation of hydrogen peroxide in plant extracts using titanium. *Analytical Biochemistry*, 139, 487–492.

Pieterse, C.M.J., Van Pelt, J.A., Ton, J., Parchmann, S., Mueller, M.J., Buchala, A.J. et al. (2000) Rhizobacteria-mediated induced systemic resistance (ISR) in *Arabidopsis* requires sensitivity to jasmonate and ethylene but is not accompanied by an increase in their production. *Physiological and Molecular Plant Pathology*, 57, 123–134.

Pozo, M.J., van der Ent, S., van Loon, L.C. & Pieterse, C.M. (2008) Transcription factor MYC2 is involved in priming for enhanced defense during rhizobacteria-induced systemic resistance in *Arabidopsis thaliana*. *New Phytologist*, 180, 511–523.

Sagi, M. & Fluhr, R. (2001) Superoxide production by plant homologues of the gp91(phox) NADPH oxidase. Modulation of activity by calcium and by tobacco mosaic virus infection. *Plant Physiology*, 126, 1281–1290.

Shan, W., Chen, J.Y., Kuang, J.F. & Lu, W.J. (2016) Banana fruit NAC transcription factor *MaNAC5* cooperates with *MaWRKYs* to enhance the expression of pathogenesis-related genes against *Colletotrichum musae*. *Molecular Plant Pathology*, 17, 330–338.

Sharma, P.C., Ito, A., Shimizu, T., Terauchi, R., Kamoun, S. & Saitoh, H. (2003) Virus-induced silencing of *WIPK* and *SIPK* genes reduces resistance to a bacterial pathogen, but has no effect on the INF1-induced hypersensitive response (HR) in *Nicotiana benthamiana*. *Molecular Genetics and Genomics*, 269, 583–591.

Sugiura, R., Toda, T., Dhut, S., Shuntoh, H., Kuno, T. & Kuno, T. (1999) The MAPK kinase Pek1 acts as a phosphorylation-dependent molecular switch. *Nature*, 399, 479–483.

Tada, Y., Spoel, S.H., Pajerowska-Mukhtar, K., Mou, Z., Song, J., Wang, C. et al. (2008) Plant immunity requires conformational charges of NPR1 via *S*-nitrosylation and thioredoxins. *Science*, 321, 952–956.

Ton, J., van Pelt, J.A., van Loon, L.C. & Pieterse, C.M.J. (2002) Differential effectiveness of salicylate-dependent and jasmonate/ethylene-dependent induced resistance in *Arabidopsis*. *Molecular Plant-Microbe Interactions*, 15, 27–34.

Tong, Z.G., Gao, Z.H., Wang, F., Zhou, J. & Zhang, Z. (2009) Selection of reliable reference genes for gene expression studies in peach using real-time PCR. *BMC Molecular Biology*, 10, 71.

Tsuda, K., Mine, A., Bethke, G., Igarashi, D., Botanga, C.J., Tsuda, Y. et al. (2013) Dual regulation of gene expression mediated by extended MAPK activation and salicylic acid contributes to robust innate immunity in *Arabidopsis thaliana*. *PLoS Genetics*, 9, e1004015.

Vallad, G.E. & Goodman, R.M. (2004) Systemic acquired resistance and induced systemic resistance in conventional agriculture. *Crop Science*, 44, 1920–1934.

Verhagen, B.W.M., Glazebrook, J., Zhu, T., Chang, H.S., van Loon, L.C. & Pieterse, C.M.J. (2004) The transcriptome of rhizobacteria-induced systemic resistance in Arabidopsis. *Molecular Plant-Microbe Interactions*, 17, 895–908.

Wang, K.T., Li, C.H., Lei, C.Y., Zou, Y.Y., Li, Y.J. & Zheng, Y.H. (2021) Dual function of *VvWRKY18* transcription factor in the β-aminobutyric acid-activated priming defense in grapes. *Physiologia Plantarum*, 172, 1477–1492.

Wang, K.T., Liao, Y.X., Xiong, Q., Kan, J.Q., Cao, S.F. & Zheng, Y.H. (2016) Induction of direct or priming resistance against *Botrytis cinerea* in strawberries by β-aminobutyric acid and their effects on sucrose metabolism. *Journal of Agricultural and Food Chemistry*, 4, 5855–5865.

Wang, K., Wu, D., Bo, Z., Chen, S.I., Wang, Z., Zheng, Y. et al. (2019) Regulation of redox status contributes to priming defense against *Botrytis cinerea* in grape berries treated with β-aminobutyric acid. *Scientia Horticulturae*, 244, 352–364.

Wu, C., Shan, W., Liang, S., Zhu, L., Guo, Y., Chen, J. et al. (2019) *MaMPK2* enhances *MabZIP93*-mediated transcriptional activation of cell wall modifying genes during banana fruit ripening. *Plant Molecular Biology*, 101, 113–127.

Xiao, S. & Chye, M.L. (2011) Overexpression of Arabidopsis ACBP3 enhances NPR1-dependent plant resistance to *Pseudomonas syringe* pv. *tomato* DC3000. *Plant Physiology*, 156, 2069–2081.

Yao, Y., He, R.J., Xie, Q.L., Zhao, X.H., Deng, X.M., He, J.B. et al. (2017) ETHYLENE RESPONSE FACTOR 74 (ERF74) plays an essential role in controlling a respiratory burst oxidase homolog D (RbohD)-dependent mechanism in response to different stresses in *Arabidopsis*. *New Phytologist*, 213, 1667–1681.

Zhang, H., Li, D., Wang, M., Liu, J., Teng, W., Cheng, B. et al. (2012) The *Nicotiana benthamiana* mitogen-activated protein kinase cascade and WRKY transcription factor participate in Nep1 (Mo)-triggered plant responses. *Molecular Plant-Microbe Interactions*, 25, 1639–1653.

Zhang, Y., Fan, W., Kinkema, M., Li, X. & Dong, X. (1999). Interaction of NPR1 with basic leucine zipper protein transcription factors that bind sequences required for salicylic acid induction of the *PR-1* gene. *Proceedings of the National Academy of Sciences USA*, 96, 6523–6528.

Zhang, Y.Y., Zhu, H.Y., Zhang, Q., Li, M.Y., Yan, M., Wang, R. et al. (2009) Phospholipase Dα1 and phosphatidic acid regulate NADPH oxidase activity and production of reactive oxygen species in ABA-mediated stomatal closure in *Arabidopsis*. *The Plant Cell*, 21, 2357–2377.

Zhou, J., Xia, X.J., Zhou, Y.H., Shi, K., Chen, Z. & Yu, J.Q. (2014) RBOH1-dependent H_2O_2 production and subsequent activation of MPK1/2 play an important role in acclimation-induced cross-tolerance in tomato. *Journal of Experimental Botany*, 65, 595–607.

Zimmerli, L., Métraux, J.P. & Mauch-Mani, B. (2001) β-aminobutyric acid-induced protection of *Arabidopsis* against the necrotrophic fungus *Botrytis cinerea*. *Plant Physiology*, 126, 517–523.

Zipfel, C. & Robatzek, S. (2010) Pathogen-associated molecular pattern-triggered immunity: veni, vidi…? *Plant Physiology*, 154, 551–554.

SUPPORTING INFORMATION

Additional Supporting Information may be found online in the Supporting Information section.

How to cite this article: Li, C., Wang, K., Huang, Y., Lei, C., Cao, S., Qiu, L., et al (2021) Activation of the BABA-induced priming defence through redox homeostasis and the modules of TGA1 and MAPKK5 in postharvest peach fruit. *Molecular Plant Pathology*, 22, 1624–1640. https://doi.org/10.1111/mpp.13134